CONF-910134--2

DE91 007703

ornl

OAK RIDGE
NATIONAL
LABORATORY

PHYSICS
DIVISION
PREPRINT

Angular momentum effects in subbarrier fusion

M. L. Halbert and J. R. Beene
Oak Ridge National Laboratory, Oak Ridge, Tennessee 37831

Invited talk at
XIV Nuclear Physics Symposium, Cuernavaca, Mexico,
January 7-10, 1991

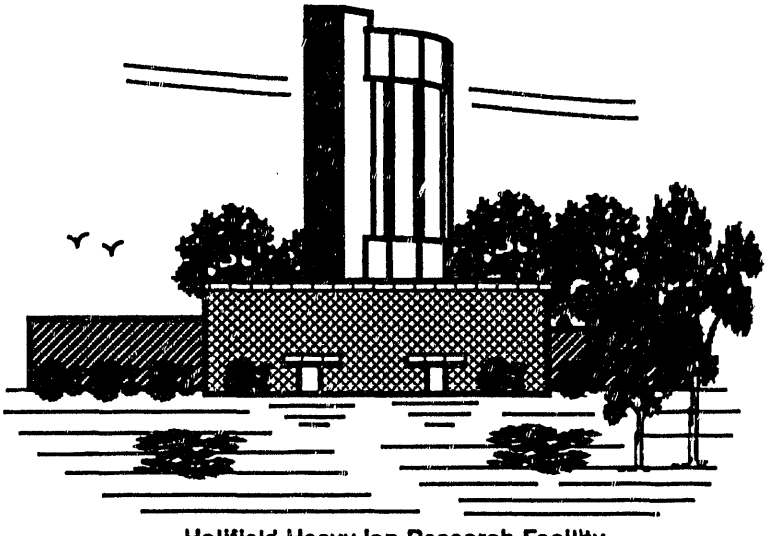

Holifield Heavy Ion Research Facility

Angular momentum effects in subbarrier fusion

M. L. Halbert and J. R. Beene
Oak Ridge National Laboratory, Oak Ridge, Tennessee 37831

ABSTRACT

Analyses of published experimental data leading to angular-momentum distributions for subbarrier fusion of ^{64}Ni and ^{100}Mo have been re-examined, especially in the low-ℓ region. Our previous results are substantially unchanged.

INTRODUCTION

In Ref. 1, the compound-nucleus angular-momentum distribution, σ_ℓ vs. ℓ, for near-barrier and subbarrier fusion of ^{64}Ni and ^{100}Mo was deduced from experimental data on γ-ray multiplicities in coincidence with Ge photopeaks characteristic of the 2n, 3n, 4n, and α2n evaporation residues. The method is well suited to the high-ℓ region, say $\ell \gtrsim 10$. However, certain complications in the data acquisition and the analysis made it difficult to reach firm conclusions about the shape of the low-ℓ portion of the σ_ℓ distribution. The main purpose of this paper is to supplement Ref. 1 with a deeper investigation of the low-ℓ region. A few other matters are also touched upon including a slight revision of the ^{64}Ni + ^{100}Mo cross sections and some data on ^{16}O + ^{148}Sm leading to the same compound nucleus, ^{164}Yb.

A. ℓ distributions

The first step in constructing angular-momentum distributions, σ_ℓ vs. ℓ, was to obtain the number k of γ rays detected in the NaI elements for each valid Ge trigger. Neutron rejection was accomplished by time of flight with reference to the zero time, t_0, of a given event, determined by the average of the NaI times as described in Ref. 1. Events with $k < 3$ did not provide a sufficiently good estimate of t_0 and were discarded in Ref. 1, possibly leading to a loss of data for certain evaporation channels populating mainly low-ℓ entry states (particularly the 4n channel at $E_{c.m.}$ = 141.7 MeV and the 3n channel at 130.1 MeV). To compensate for the supposed loss, a constant-T_ℓ extrapolation was made in Ref. 1 from the peak region of each σ_ℓ distribution down to $\ell = 0$.

We have now generated new k distributions at $E_{c.m.}$ = 130.1 and 141.7 MeV by a scan of the primary data tapes without $k < 3$ rejection or any attempt to reject NaI pulses due to neutrons. The gate on NaI times was wide enough to insure that no pulses due to

prompt γ rays were excluded. Figure 1 shows the resulting "unfiltered" k distribution (dots) for the 4n channel at 141.7 MeV in comparison with the result of a scan of the same original data tape, but with neutrons and $k < 3$ events filtered out as in Ref. 1. (Each set of data in Fig. 1 is a net distribution after background subtraction; i.e., the k distribution in coincidence with Ge pulses appearing in the photopeak of the $2^+ \rightarrow 0^+$ transition of ^{160}Yb, minus the k distribution in coincidence with a gate on nearby portion of the Ge spectrum.) One notes in Fig. 1 that the shape of the peak and the region above it are nearly the same, with the unfiltered data apparently shifted up by a few units of k due to the detection of neutrons. In Fig. 2(c), the same data are replotted with one distribution shifted by 2.5 units to achieve the best match on the high side of the peak; this best match is uncertain by about ± 0.5 units of k. Also shown in Figs. 2 and 3 are k distributions for the other neutron-evaporation channels at these two energies. The best-fit shifts are 2.5 ± 0.5 for the 3n and 4n channels at 141.7 MeV and 2.0 ± 0.5 for the other three sets of data. These shifts in k per neutron, averaged over the five sets of data, correspond to 0.8 ± 0.3 NaI detectors triggered by each evaporated neutron. The primary triggering efficiency for a single NaI detector has been measured to be 0.45 to 0.50 for evaporation neutrons.[2] The excess probability of neutron detection seen here is no doubt due to scattering of neutrons from one NaI crystal to another. A neutron that scatters in a given NaI is likely to be deflected from its original direction and has a better chance of interacting with additional NaI crystals since it will most likely traverse more NaI after deflection than it would have without such a deflection.

Figures 2(c) and 3(b) show that the filtering rejected some of the low-k events besides those with $k < 3$. This had no effect on the absolute cross sections since they were already determined from the yields of the Ge photopeaks without any k selection (see Section B below). However, the filtering might have had some effect on the shape of σ_ℓ for fusion, since σ_ℓ is constructed from the sum of ℓ distributions of all the exit channels. If the neutron detection probability is 0.8 ± 0.3, the extra counts at low k which might be due to γ rays cause a decrease in the mean ℓ of 1.7 ± 2.1 units at 141.7 MeV and 0.9 ± 1.6 at 130.1 MeV. (These estimates assume that a change of one unit in k results in a change of two units in ℓ.) The constant-T_ℓ extrapolations of Ref. 1 overestimated the losses due to the filtering and resulted in larger decreases in $\langle\ell\rangle$, namely 2.2 and 2.5, respectively. Thus the net effect of abandoning the extrapolations and including the $k < 3$ events (after correcting as above for neutron detection) is an *increase* of $\langle\ell\rangle$ over the values in Ref. 1. In particular, $\langle\ell\rangle$ increases from 28.4 to 28.9 ± 2.1 at 141.7 MeV and from 18.4 to 20.0 ± 1.6 at 130.1 MeV. These increases in $\langle\ell\rangle$ are $(2 \pm 7)\%$ and $(9 \pm 8)\%$, respectively, comparable to the errors on $\langle\ell\rangle$ estimated in Ref. 1. The conclusion to be drawn here is that our present analysis gives results for $\langle\ell\rangle$ consistent with (or a few percent larger than) those published earlier.[1] Thus the discrepancy between the experimental results and the predictions of the barrier-penetration or coupled-channels theories is confirmed and may even be slightly worse.

B. Cross sections

The absolute cross sections were based on Ge photopeak yields of the $2^+ \rightarrow 0^+$ transitions in the 2n, 4n, and α2n evaporation residues, and the $17/2^+ \rightarrow 13/2^+$ transition

in the 3n product. For some of the data, the Ge pulses were recorded without regard for the number, k, of NaI detectors that had been triggered in each event. However, for the majority of the primary data tapes, events with $k = 0$ were not recorded in order to avoid filling the tapes with large numbers of Coulomb-excitation events.

We have made new Ge spectra by scans of the few primary tapes (10% of the total) which did include the $k = 0$ events, and have compared them with similar spectra from scans of primary tapes that suppressed these events. Within the statistical uncertainty of 3-12%, arising mainly from uncertainties in the background subtraction, there is no loss of evaporation-residue γ rays due to the $k > 0$ requirement. The absolute cross sections of Ref. 1 are thus unchanged on this account.

However, two other effects have been found to modify the published[1] cross sections slightly. (1) False vetoes of valid events may be generated by the NaI Compton suppressors surrounding each Ge counter. Consider an event with a valid full-energy pulse in one of the Ge counters. If by chance its Compton suppressor registers a different γ ray or a neutron from the same event, this event would be rejected. The fraction of such false vetoes, estimated from the geometry and the NaI efficiency for γ ray and neutron detection, was about 3 to 10% depending on the γ-ray and neutron multiplicity for the various exit channels. The published[1] cross sections should be increased on this account. (2) The fusion cross sections of Ref. 1 were not based on the sum of the exit-channel cross sections as stated in Ref. 1. Actually, they were taken from the area of the constant-T_ℓ extrapolations from the peak region of σ_ℓ down to $\ell = 0$ since these extrapolations were thought[1] to provide an approximate compensation for the supposed losses at low k due to the $k < 3$ rejection. (The 7 to 11% supplement for weak channels[1] was then added to these areas.) In view of the present demonstration that the supposed losses were in fact very small, the extrapolations gave an overestimate of σ_{fus}. The net effect of (1) and (2) together requires a reduction of the σ_{fus} in Ref. 1 by 10 to 30% depending on bombarding energy. These changes in σ_{fus} are insignificant compared with the order-of-magnitude discrepancies noted in Ref. 1 between experiment and various theories, and none of the conclusions of Ref. 1 is changed.

C. Angular-momentum removal at small ℓ

The experimental σ_ℓ vs ℓ distributions for fusion that are presented in Ref. 1 tend to be concave on the low-ℓ side rather than showing a $2\ell+1$ dependence. This may be traceable to approximations made in the multiplicity-to-ℓ transformation. In Ref. 1, the angular momentum removed per evaporated particle or per statistical γ ray was taken to be the average over all ℓ values for that channel. For initial states of low ℓ, this approximation may not be accurate enough; in fact, statistical γ-ray transitions from states with $\ell \sim 0$ can lead to final states of higher spin.

We have investigated the ℓ dependence of angular-momentum removal with the statistical model[3] parameterized as described in Ref. 1. The decay of many ^{164}Yb compound nuclei, each having a single ℓ value, was followed in the cascades to the various final products. Figure 4 shows the average spin removed per neutron, ΔJ_n, and

per statistical γ ray, ΔJ_s, as a function of compound-nucleus angular momentum, ℓ, for an initial excitation energy (49.4 MeV) corresponding to formation of ^{164}Yb by ^{64}Ni + ^{100}Mo at $E_{c.m.}$ = 141.7 MeV. Also shown is the average number, M_s, of statistical γ rays per event. The negative values of ΔJ at low ℓ indicate that the spin increases. It is clear that ΔJ_n has a strong ℓ dependence and ΔJ_s has a significant one, but M_s varies only by about 5-10%. (We should mention that the M_s and ΔJ_s shown in Fig. 1 include only the E1 component of the γ decays; the M1 and non-yrast E2 were assumed to be negligible. This assumption may not be valid and is under study at present.)

Figure 5 compares σ_ℓ vs ℓ for ^{64}Ni + ^{100}Mo fusion at $E_{c.m.}$ = 141.7 MeV calculated with the channel-by-channel M to ℓ transformation [Eq. (1) of Ref. 1] using the ℓ-dependent functions (full curves) or the average values used previously[1] (dashed curves). These curves represent the sum of the 2n, 3n, 4n, and α2n exit-channel ℓ distributions. (The predicted ℓ distributions for the many weak exit channels not observed in the experiment sum to a curve of very similar shape, so their omission here should not distort the shape of σ_ℓ significantly.) The more realistic calculations, those taking into account the ℓ dependence, give broader ℓ distributions and approach the expected 2ℓ+1 behavior more closely. However, these calculations omit an effect alluded to in Ref. 1, namely that the experimental data for the important 3n channel are biased against entry states of small spin because these data were obtained from a gate on the $17/2^+ \rightarrow 13/2^+$ transition in ^{161}Yb; this may account for some of the remaining concavity at small ℓ.

D. Unitarity limit

Another check on the low-ℓ magnitude of σ_ℓ is available, namely a comparison with the limit on σ_ℓ imposed by unitarity, i.e., $T_\ell = 1$ in the general relation

$$\sigma_\ell = \pi\lambda\!\!\!^{-2}(2\ell+1)T_\ell. \qquad (1)$$

The ^{64}Ni + ^{100}Mo data do not provide a useful check because even at the highest relative energy studied here, barrier penetration is substantially below the $T_\ell = 1$ limit for all ℓ. However, measurements[1] of ^{16}O + ^{148}Sm (same compound system), made immediately after the ^{64}Ni bombardments and analyzed in exactly the same way, do provide a useful check. The ^{16}O bombarding energies were E_{beam} = 71.2 and 81.3 MeV.

The higher ^{16}O energy is about 20% above the Coulomb barrier and therefore σ_ℓ should reach the unitarity limit at low ℓ. Figure 6 compares σ_ℓ with the unitarity limit (dashed line) with the sum of the σ_ℓ for the four principal channels (full line). The statistical model predicts that the weak channels undetected in the experiment combine to give an additional 12.6% yield with essentially the same ℓ distribution as the sum of the dominant channels. The dotted line in Fig. 6 shows the experimental σ_ℓ distribution increased by 12.6%, which brings the low-ℓ region very close to the unitarity limit, certainly within the 15% uncertainty of the absolute normalization. The above remarks on

the role of the $17/2^+ \rightarrow 13/2^+$ gate apply here also as a possible explanation of the concavity at the lowest ℓ values.

As mentioned above, the same apparatus and method of analysis were used for both the O + Sm and Ni + Mo data; the agreement of the O + Sm data with the unitarity limit makes us confident that the low-ℓ cross sections for Ni + Mo cannot be significantly larger than those given in Ref. 1.

E. Summary

We have re-analyzed the low-ℓ region of the σ_ℓ vs ℓ distributions published in Ref. 1, omitting efforts at neutron rejection and taking into account several subtle effects that had been previously ignored. We have found that the previously adopted extrapolation to $\ell = 0$ overestimates the low-ℓ cross section. Overall, the new analysis shows slight *increase* in the average ℓ and small decreases in the magnitude of σ_{fus}, neither of which changes the previously reported[1] discrepancies of the data with predictions by coupled-channels calculations or barrier-penetration models. Comparison with the limit imposed by unitarity showed that there was no loss of cross section at low ℓ values.

ACKNOWLEDGEMENTS

We thank D. C. Hensley, K. Honkanen, T. M. Semkow, V. Abenante, D. G. Sarantites, and Z. Li for their participation in the experimental data acquisition and the original analysis. We also wish to thank D. Schwalm, C. Dasso, and R. Vandenbosch for comments on Ref. 1 which led to the further investigations reported here. Oak Ridge National Laboratory is managed by Martin Marietta Energy Systems, Inc. under contract DE-AC05-84OR21400 with the U.S. Department of Energy.

REFERENCES

1. M. L. Halbert, J. R. Beene, D. C. Hensley, K. Honkanen, T. M. Semkow, V. Abenante, D. G. Sarantites, and Z. Li, Phys. Rev. C **40**, 2558 (1989).
2. Z. Majka, N. Abenante, Z. Li, N. G. Nicolis, D. G. Sarantites, T. M. Semkow, L. G. Sobotka, D. W. Stracener, J. R. Beene, D. C. Hensley, and H. C. Griffin, Phys. Rev. C **40**, 2124 (1989).
3. A. Gavron, computer code PACE2, Phys. Rev. C **21**, 230 (1980); and private communication; J. R. Beene, computer code modification PACE2S.

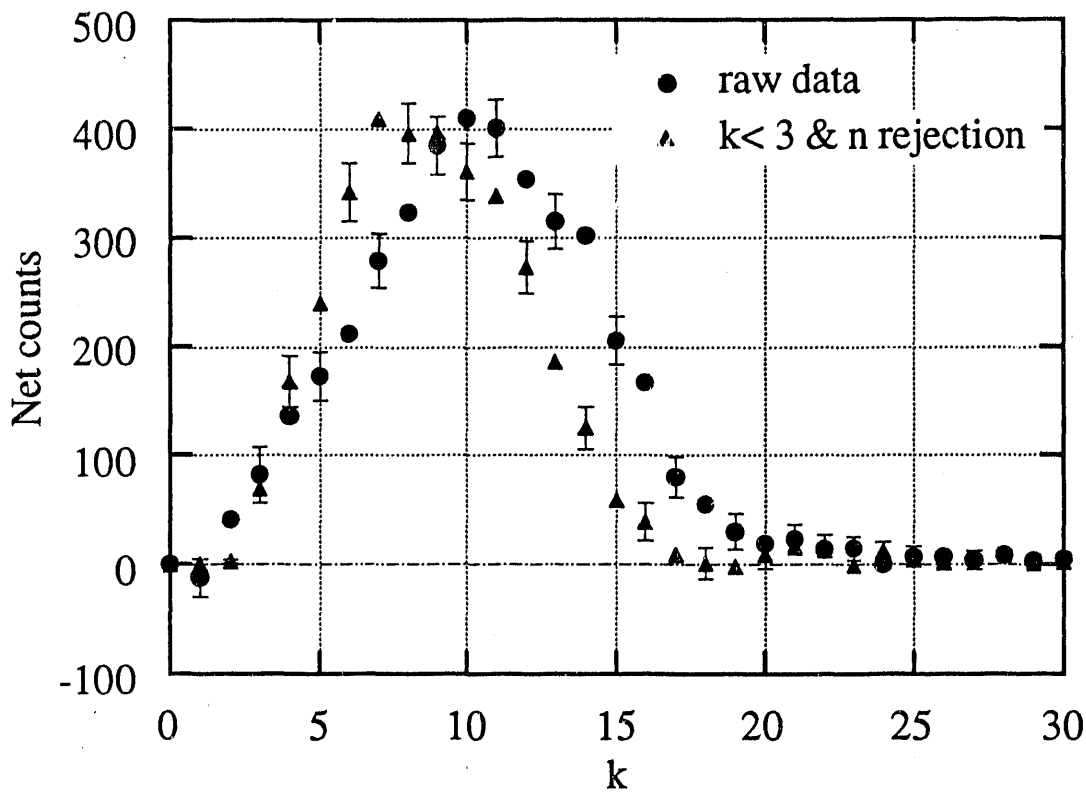

Fig. 1. Distribution of the number, k, of NaI detectors responding per event for the 4n channel at $E_{c.m.}$ = 141.7 MeV. The dots are for a sample of data taken with all k values accepted and no neutron rejection. The triangles are the same data subjected to a filter that rejected all events with $k < 3$ and any late-arriving NaI pulses, presumably due to neutrons.

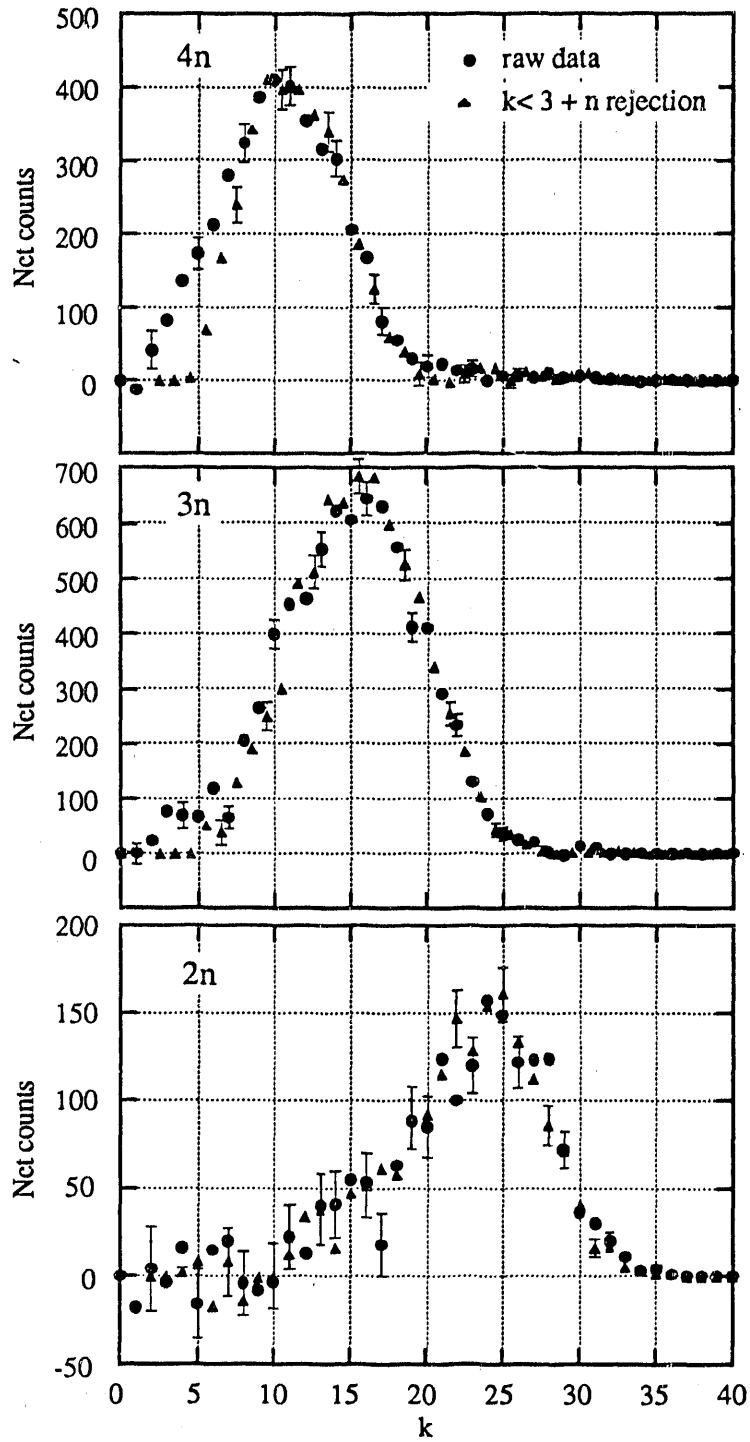

Fig. 2. Same as Fig. 1 except that the filtered data (triangles) have been shifted to higher k to obtain the best match of the peak region and above. Three exit channels are shown here: (a) 2n, (b) 3n, (c) 4n.

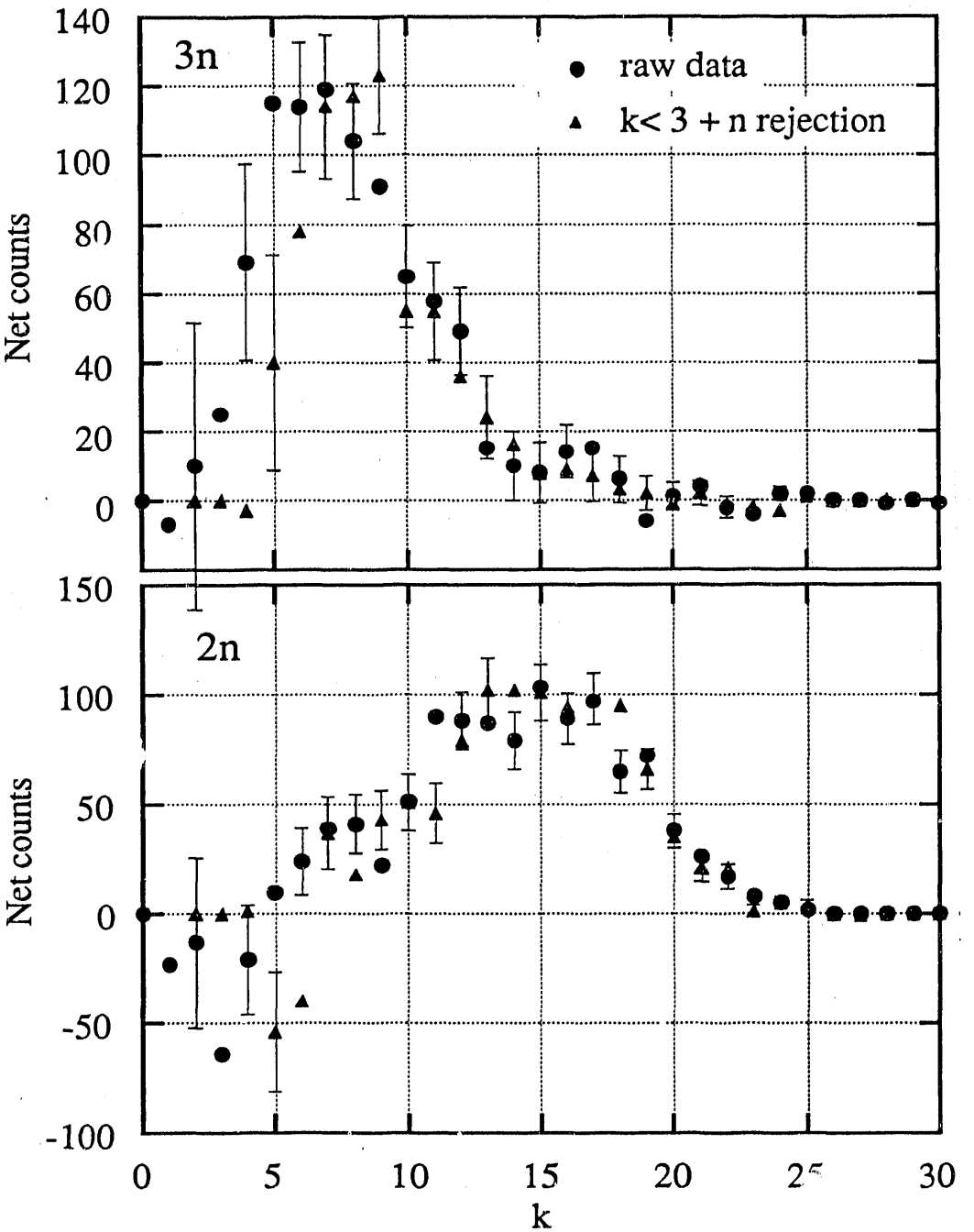

Fig. 3. Same as Fig. 2 except that the data are for the exit channels (a) 2n, (b) 3n at $E_{c.m.}$ = 130.1 MeV.

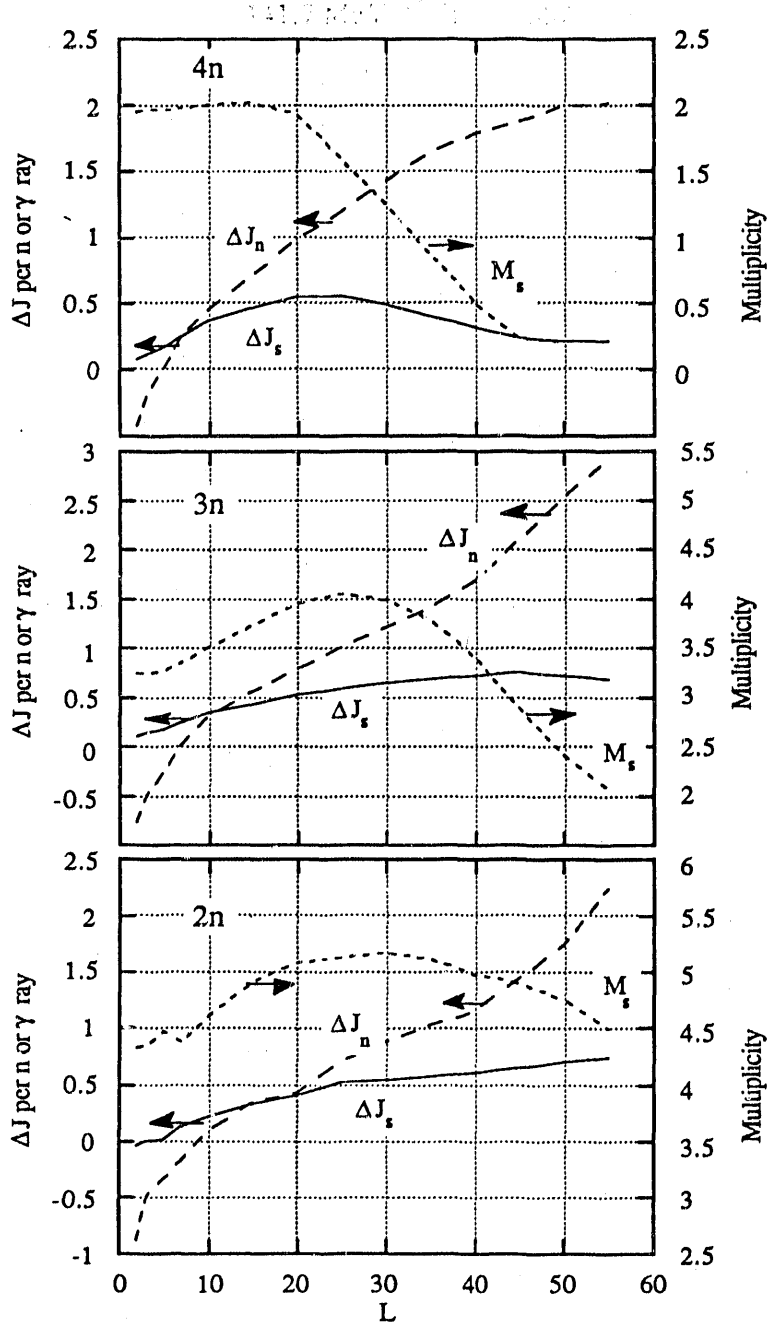

Fig. 4. Angular-momentum dependence of angular momentum removed by evaporation of a neutron, ΔJ_n (dots), or a statistical γ ray, ΔJ_S (triangles), for the 2n, 3n, and 4n channels at $E_{c.m.}$ = 141.7 MeV, as calculated with the statistical model. Also shown (by the right-hand scale) is the statistical γ-ray multiplicity, M_S.

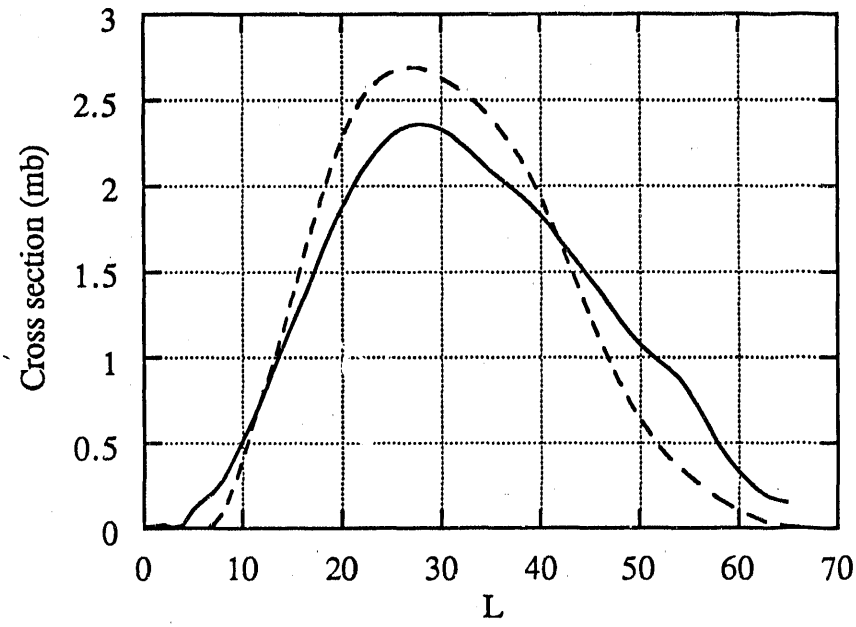

Fig. 5. Two σ_ℓ vs ℓ distributions deduced from the same channel-summed experimental M distribution for $^{64}Ni + {}^{100}Mo$ fusion at $E_{c.m.}$ = 141.7 MeV. The full curve is from a transformation made with ℓ-dependent parameters for angular momentum removal while the dashed curve was obtained by using the corresponding values averaged over ℓ, as in Ref. 1.

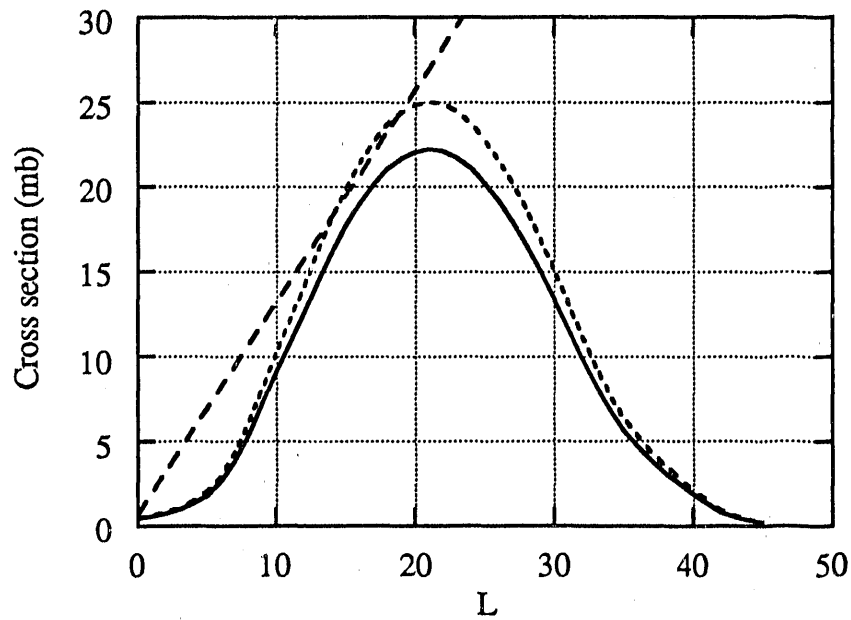

Fig. 6. Comparison of ℓ distribution deduced from experimental data on $^{16}O + {}^{148}Sm$ at $E_{c.m.}$ = 72.5 MeV (full curve) with the unitary limit (dashed). The dotted curve shows the experimental curve scaled up by 12.6% to take account of the unobserved channels (see text).

END

DATE FILMED

03/05/91